

# HYBRID LEARNING APPROACH FOR FEATURE EXTRACTION AND CLASSIFICATION IN HYPERSPECTRAL IMAGES

Murali Kanthi

Department of Computer Science and Engineering, JNTU College of Engineering Anantapuram,  
Anantapur, Andhra Pradesh, India.  
murali.kanthi@gmail.com

T. Hitendra Sarma

Department of Information Technology, Vasavi College of Engineering, Hyderabad, Telangana, India.  
hitendrasarma@ieee.org

C. Shoba Bindu

Department of Computer Science and Engineering, JNTU College of Engineering Anantapuram,  
Anantapur, Andhra Pradesh, India.  
shobabindhu@gmail.com

## Abstract

Hyperspectral Images (HSI) provide a rich set of spatial and spectral information that is used for the classification of the HSI dataset. The large-scale hyperspectral image data leads to many processing challenges for the conventional data analysis techniques. To minimize the computational complexity and enhance the classification performance of the HSI dataset, we presented a new hybrid learning technique for feature extraction and classification (Hybrid-LN) model in this work. It is a simple two-step approach, to reduce computational complexity, the first step is applied to generate a spatial-spectral reduced HSI dataset by identifying the most significant pixels from each class and the most significant bands of the HSI. To increase HSI classification performance, the second step involves training a CNN to extract spatial-spectral features from the reduced HSI. Results from three benchmark HSI datasets - Salinas scene (SA), Indian Pines (IP), and Pavia University scene (PU)- are compared to those from the current models. Experimental results show that the computational complexity of the proposed approach is significantly reduced and producing relatively good classification accuracy with the state-of-the-art methods.

**Keywords:** Hyperspectral Image, Spatial and spectral information, Classification, CNNs.

## 1. Introduction

Hyperspectral Images (HSI) contain a large volume of data with more detailed information in more bands (usually in hundreds). Classification of Pixels in HSI is a challenging problem due to its high dimensionality and availability of very limited reference data. Hyperspectral Image analysis has potential applications in climate monitoring, crop health monitoring, mineral exploration, health care, and security, etc [Dias *et al.*, (2013)]. In HSI, every pixel contains the information of several objects on the ground. Pixel classification is a fundamental activity in the HSI analysis. Both supervised and unsupervised methods are well explored in recent years to analyze the HSI data. Due to the limited availability of labeled data and high dimensionality the conventional classification methods like Support Vector Machine, Naïve Bayes, K-Nearest Neighbor methods are less efficient. However, some successful attempts are made to improve these methods for HSI data analysis [Cariou *et al.*, (2020); Okwuashi *et al.*, (2020)]. The classification of these methods depends on the feature extraction or selection methods applied in the reprocessing stage. Most significantly, both spatial and spectral information must be taken into account when selecting or extracting features.

Dimensionality reduction is a crucial step to achieve better classification accuracy [Xu *et al.*, (2019), Cao *et al.*, (2019), Aria *et al.*, (2020)]. Deep Learning approaches have become more popular in recent years particularly in the field of remote sensing. Methods based on convolutional neural networks (CNNs) have been used to classify hyperspectral images. To extract spectral-spatial information and enhance classification accuracy, 2D CNN and 3D CNN are presented [Paoletti *et al.*, (2019), Hamouda *et al.*, (2020)]. In these methods, 3D convolution filters extract spectral-spatial characteristics together, whereas 2D convolution filters extract spectral-spatial characteristics independently. Here, 3D Feature extraction approaches proved to be more efficient than 2D models. But, when the computational resources are limited, it requires high computation cost to train the 3D-CNN model because of more spectral dimensions in the HSI. Almost all the recent CNN architectures can provide more than 95% classification accuracy on the publicly available benchmark datasets. However, these methods require more high-quality sample pixels for optimal model learning. Further, they also require high computational resources for training. Unsupervised learning (clustering) methods on the other hand need a little prior information about the ground truth for grouping similar pixels or bands. This may then be used to learn spatial-spectral features [Wei *et al.*, (2019)]. Using clustering approaches, a number of dimensionality reduction, band selection, and feature extraction strategies have been implemented [Datta *et al.*, (2012), Yao *et al.*, (2020), Bianca *et al.*, (2020)]. Clustering techniques are also used in solving the spectral unmixing problem [Xu *et al.*, (2014)]. The most commonly used clustering approach is k-means which is extensively studied and applied in many recent works on Hyperspectral Image Analysis such as band reduction [Kumar *et al.*, (2014)], spectral unmixing [Xu *et al.*, (2014)], and segmentation [Kennedy *et al.*, (2020)]. Because of the huge volume of data and high computational requirements, recent studies are focusing to develop fast classification techniques without compromising the classification accuracy [Wei *et al.*, (2019)]. Approximating spectral clustering is a key to make the learning algorithms more scalable and faster [Tremblay and Loukas, (2020)]. Both theoretically and experimentally the importance of spectral clustering [Challa *et al.*, (2020)] motivates a new scope to develop scalable and fast classification methods for HSI analysis [Liu *et al.*, (2020), Yuan and Zhu, (2020)]. This paper presents a simple and hybrid learning method for classification of pixels in the HSI. The proposed method runs in two stages. To reduce computational complexity, the first step is applied to generate a spatial-spectral reduced HSI dataset by identifying the most significant pixels from each class and the most significant bands of the HSI. To increase HSI classification performance, the second step involves training a CNN to extract spatial-spectral information from the reduced HSI. Results from three benchmark HSI datasets are compared to those from the current models. The computational complexity of the suggested technique is considerably decreased, resulting in reasonably excellent classification accuracy in comparison to state-of-the-art approaches, according to the findings of the experiments.

The following is a list of the paper's key contributions.

- A spatial clustering approach is presented to select significant pixels from each class using k-means clustering to create spatially reduced HSI.
- A spectral clustering approach is proposed for reducing the redundant spectral bands from the spatially reduced HSI by applying above said k-Means algorithm to reduce the computational complexity.
- A CNN-based feature learning approach is proposed for extracting the features from the reduced HSI and fully connected layers are employed to classify the HSI for different class labels.

The rest of this paper is laid out as follows. The research that are relevant to the proposed study are presented in Section 2, Section 3 describes the suggested model which consists of two more subsections including clustering-based feature learning and CNN-based classification. Section 4 presents the experimental study which includes data description, experimental setup, and classification results. Finally, in Section 5, the findings are given.

## 2. Related Work

With the feature of "joint spectral-spatial information", the HSI data cube provides extensive spatial and spectral information. Between the bands, there is a significant connection. As a result, dealing with big dimensional data becomes a complex method and a difficult challenge; in this light, HSI data reduction is seen as critical job. This section gives an overview of contemporary data reduction approaches in HSI, including spatial reduction, spectral reduction (dimensionality reduction), or a combination of the two. In general, HSI dimensionality

reduction approaches may be divided into two groups: feature extraction and feature selection. With feature extraction, the original HSI is converted into a lower-dimensional space, resulting in a smaller dataset. While certain discriminatory bands are chosen to represent the original HSI for band selection.

According to [Li *et al.*, (2017)] CNN-based approaches outperformed stacked autoencoder and deep brief network-based approaches in classification. To exploit the intraclass and inter-class structure information, [Hao *et al.*, (2017)] presented class-wise dictionary learning model for HSI classification with manifold regularizes. [Yu *et al.*, (2017)] developed a CNN model to enhance its discriminative power for HSI classification, in which the original data is utilized as input and the final CNN outputs are projected class results using hand-crafted features. A feature extraction method supported Siamese CNN is presented by [Liu *et al.*, (2017)] to enhance performance of HSI classification within the situation that a couple of labeled samples are available for training.

[Paoletti *et al.*, (2018)] stated that HSI faces some challenges, associated with the processing of high-dimensional information. This leads to a big increase in computation time. [Chen *et al.*, (2018)] presented a technique for enhancing the effectiveness of HSI classification by combining spectral and spatial information from HSI and using an adaptable method for selecting the spatial window. There is an explicitly nonlinear translation for effective feature learning and concrete learning techniques used to extract distinct topologies of HIS data to accomplish nonlinear dimension reduction presented by [Zhang *et al.*, (2019)]. The overwhelming characteristics produced from the original 3D CNN model suffer from overfitting and greater training cost, according to [Yu *et al.*, (2020)]. To exploit spatial context and spectral correlation, [Azar *et al.*, (2020)] presented sparse modeling approach for HSI classification. Spectral blocks and spatial groups are combined to utilize the HSI's spectral and spatial redundancy to solve high-dimensional optimization issues. In order to reduce the issue of HSI classification having spatial diffusion, [Fang *et al.*, (2020)], It uses a weighted Gaussian mask to learn spatial features. It was designed to decrease the number of noisy and unnecessary spectral bands. [Bianca *et al.*, (2020)] presented a model for reducing the classification time with exploiting various algorithms on real hyperspectral data sets to find out which algorithm is more effective.

[Datta *et al.*, (2012)] offer an unsupervised band selection technique for HSI, in which the bands are rated based on their classification discriminating abilities. For HSI applications, [Yuan *et al.*, (2016)] presented a multigraph determinantal point process approach to successfully identify a variety of band combinations that comprise discriminative and informative bands. Ensemble clustering techniques are also proposed in [Wu *et al.*, (2017)] to choose the most recognizable band of HSI, which alleviates the computation burden and improves cluster performance. Some scalable and optimal clustering and classification methods for HSI data are presented in [Wang *et al.*, (2018), Xie *et al.*, (2018), Zhao *et al.*, (2019)]. ClusterCNN is a two-stage classification approach introduced by [Yao *et al.*, (2020)], in which the first phase separates HSI pixels into various groups to produce a material map. The second stage involves training a CNN to extract spatial characteristics from the material map, which is then used to classify HSI pixels. [Hosseini *et al.*, (2020)], introduced a new method to capture spectral fluctuations by simplifying reflectance using unsupervised dimensionality reduction.

As summarized in the above short review of the recent works in the literature, most of the recent studies have suggested that both supervised and unsupervised learning approaches are important to enhance classification performance by extracting spectral-spatial features while dealing with large-scale HSI data. Hence, the current work is motivated to develop a new hybrid learning network (Hybrid-LN) for HSI classification. This will be discussed in more detail in the next sections.

### 3. Proposed Hybrid Learning Network (Hybrid-LN) Model

This section presents details of the proposed Hybrid Learning Network (Hybrid-LN) Method. As shown in Figure 1, the presented model applies both unsupervised (k-means clustering method) and supervised (CNN Classifier) methods. It runs in two stages. To reduce computational complexity, the first step is applied to generate a spatial-spectral reduced HSI dataset by identifying the most significant pixels from each class and the most significant bands of the HSI. The second step is used to train a CNN to enhance the HSI classification performance by extracting spatial-spectral information from the reduced HSI. Sections 3.1 and 3.2 presents the Cluster-based feature learning and the CNN-based classification approaches.

#### 3.1. Cluster-based feature learning

The hyperspectral image contains a lot of spatial information and also has a high of spectral dimensions. Preprocessing of the hyperspectral image is necessary to minimize the spatial size without losing spatial information, as well as to pick the appropriate bands to reduce classification processing time, which is critical when computing resources are limited. The suggested hybrid model for spatial and spectral reduction of HSI data to increase classification accuracy and minimize computing cost is presented in this part. The details of spatial and spectral clustering are provided in the sub-sections below.

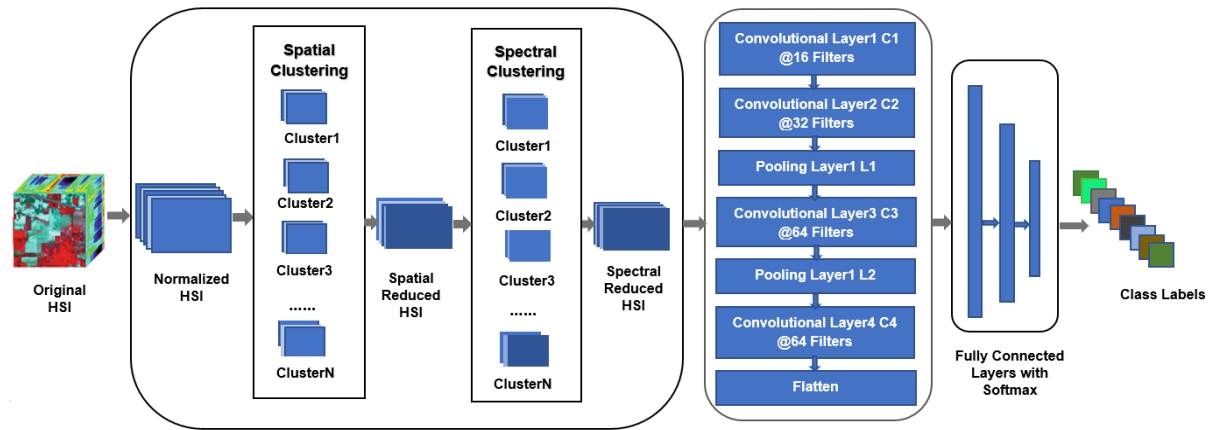


Fig. 1. An overview of the proposed hybrid learning network (Hybrid-LN) model

### 3.1.1. Spatial clustering

Let the original HSI dataset be  $X \in \mathbb{R}^{W \times H \times B}$  and the corresponding ground truth image as  $Y \in \mathbb{R}^{W \times H}$ , where  $W \times H$  is the spatial information and  $B$  is the spectral bands of the image, respectively. The conventional k-means clustering algorithm is modified to do the clustering both spatially and spectrally over the given HSI. In this study, the number of clusters ( $k$  value) is taken from the available ground truths. Initially, the k-means clustering is used to divide the pixels (spatial clustering) into ' $k$ ' distinct groups. Each group is represented by its mean. To reduce the size of the HSI spatially, a fixed percentage, say  $p$ , of pixels, are identified based on their closeness to its center from each cluster  $C_i$ . To avoid an empty cluster problem, if the  $|C_i| < p$ , then all the pixels in  $C_i$  are selected into the reduced HSI data. The spatial clustering algorithm 1 provides the most significant pixels from each class to get a spatial reduced HSI denoted by  $X'^{w \times b}$ , where  $w$  is the pixels chosen in the preceding procedure.

#### Algorithm 1. Spatial clustering: k-means ( $X, k$ )

1. Apply k-means algorithm on  $X$  to create  $k$  no. of disjoint clusters, say  $C_1, C_2, C_3, \dots, C_k$
2. Let  $i = 0$ ; /\*  $i$  is the iteration counter \*/
- repeat**
3.  $i = i + 1$ ;
- if** ( $|C_i| > P_i$ ) **then**
4. Select  $P_i$  nearest samples from the cluster center of  $C_i$  are selected and add to  $X'$
- else**
5. Select all samples from  $C_i$  and add to  $X'$
- end if**
- until** ( $i = k$ )
6. Output:  $X'^{w \times b}$

#### Algorithm 2. Spectral clustering ( $X', k$ )

1. Apply k-means algorithm on all the bands in  $X'$  to create  $k$  disjoint clusters, say  $B_1, B_2, B_3, \dots, B_k$
2. Let  $i = 0$ ; /\*  $i$  is the iteration counter \*/
- repeat**
3.  $i = i + 1$ ;
- if** ( $|B_i| > n$ ) **then**
4. Select  $n$  number of bands from cluster  $B_i$  which are closer to the center and add to  $X''$
- else**
5. Select all bands from cluster  $B_i$  and add to  $X''$
- end if**
- until** ( $i = k$ )
6. Output:  $X''^{w \times b}$

### 3.1.2. Spectral clustering

Dimensionality reduction is a necessary preprocessing step for HSI data to avoid the “curse of dimensionality” problem. In the current work, a spectral clustering using the k-means approach is proposed to select significant bands which improves the training process of the classifiers and to reduces the computational cost of the model. k-means clustering is applied on  $X'$  to get  $k$  disjoint clusters of similar spectral bands, say  $B_1, B_2, B_3, \dots, B_k$ , where  $k$  is the required number of dimensions to be reduced. Select  $n$  number of bands that are closer to the center of the cluster  $B_i$ . If  $|B_i| < n$  then add all bands to  $X''$ , to overcome the empty cluster problem. This process is repeated for each cluster to select the most significant bands to get spectrally reduced HSI data, denoted by  $X''^{w \times b}$ , where  $b$  be the bands selected in the above process, as presented in the spectral clustering algorithm.

### 3.2. CNN-based classification

Figure 1 depicts the second phase in the proposed Hybrid Learning Network (Hybrid-LN) paradigm. To produce full-size picture patches, the spatial-spectral reduced HSI data set,  $X'$ , is treated as a data matrix and zero padding is applied. The HSI data matrix is then divided into random train and test subsets. The collection of train vectors supplied as input to the first layer of the 2D-CNN model is called  $X''_{\text{Train}}$ , while the set of test vectors is called  $X''_{\text{Test}}$ . We present a 2D-CNN model that uses image patches clipped from the zero-padded matrix as input and predicts the class label for each patch's pixel center. Four convolution layers ( $C_1, C_2, C_3$ , and  $C_4$ ), two pooling layers ( $P_1$  and  $P_2$ ), three fully connected layers ( $fc_1, fc_2$ , and  $fc_3$ ), and three sets of filters  $K_1=16$ ,  $K_2=32$ , and  $K_3=64$  with  $3 \times 3$  sizes make up the suggested model. Max-pooling and batch normalization layers follow the first two convolutional layers. The max-pooling layer comes after the third convolutional layer, while the batch normalization layer comes after the last convolutional layer. Max-pooling with  $2 \times 2$  strides and ReLU activation function are applied after every convolutional layer. The batch normalization layers are utilized to boost the suggested model's performance. The output is subsequently reconfigured and delivered to layers that are fully connected. When there is a limited quantity of training data, the dropout layer is applied after each fully connected layer as a regularization technique to avoid over-fitting. Finally, using maximum function parameters, the class label can be predicted.

## 4. Experimental Study

### 4.1. Data description

Three publicly accessible benchmark HSI datasets were used to test the performance of the presented Hybrid-LN model, including the Salinas scene (SA), the Indian Pines scene (IP), and the Pavia University scene (PU). The Indian Pines (IP) dataset was gathered over the Indian Pines test site in Northwestern Indiana with 16 class labels, the ground truth is available. The Pavia University (PU) picture was acquired during a flying campaign over Pavia, northern Italy. With 9 class labels the ground truth is available. The Salinas (SA) scene was collected over Salinas Valley with 16 classes in the ground truth. Figure 2, 3, and 4 depicts a false-color maps and a ground-truth classification maps for these datasets respectively and the details are described in Table I.

Parameters	Indian Pines	Pavia University	Salinas
Spatial Dimension	$145 \times 145$	$610 \times 340$	$512 \times 217$
No. of Spectral Bands	200	115	200
No. of Classes	16	9	16
Wavelength Range	$0.4-2.5 \mu\text{m}$	$0.43-0.86 \mu\text{m}$	$360-2500 \mu\text{m}$
Sensor	AVIRIS	ROSIS	AVIRIS

Table 1. Description of popularly used benchmark Hyperspectral Image datasets.

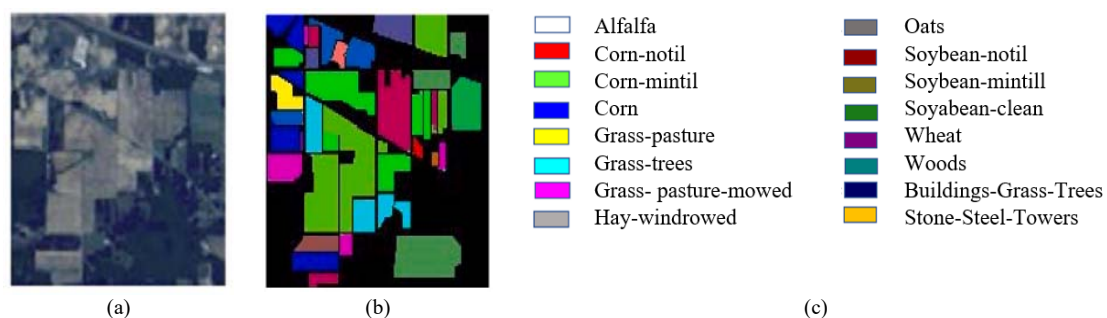


Fig. 2. IP dataset. (a) False-color map, (b) Ground-truth with reflective class legends.

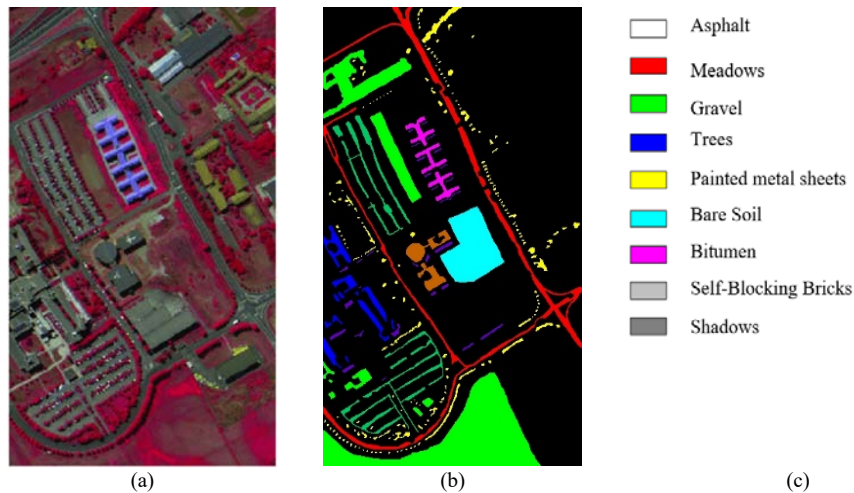


Fig. 3. PU dataset. (a) False-color map, (b) Ground-truth with reflective class legends.

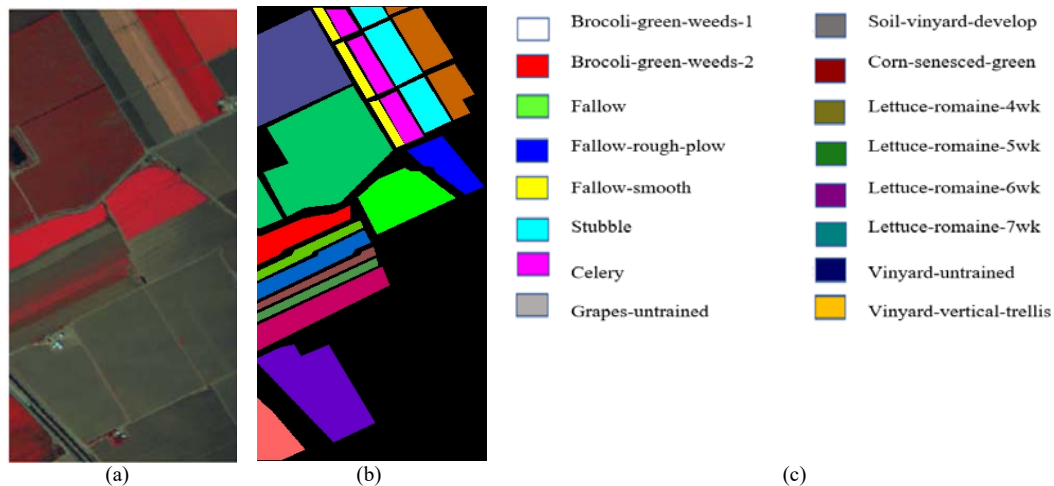


Fig. 4. SA dataset. (a) False-color map, (b) Ground-truth with reflective class legends.

#### 4.2. Experimental setup

To assess the proposed model's efficacy, it is compared to other HSI classification methods such as SVM, 2D-CNN, 3D-CNN, and SMSB in terms of well-known numerical indices, average accuracy (OA), overall accuracy (OA), and kappa statistic (K). All the experiments are conducted on the google cloud with Tesla T4 Graphical Processing Unit (GPU) having 25.51 GBRAM. The model was built using Keras-2.2.4 and Python 3.6. In the proposed model, the learning rate, batch size, dropout rate, and number of training epochs are all set to 0.001, 256, 0.4, and 200, respectively. As an input to the model, we pick a window size of 25x25. Then, to decrease the impact of random initialization, perform all of the trials five times and compute the average findings for the final classification report.

#### 4.3. Classification results

The Hybrid-LN classification is compared to several state-of-the-art HSI classification techniques such as SVM [7], 2D-CNN [7], 3D-CNN [7], and SMSB [28] to demonstrate the performance of the presented model. To produce a reduced HSI dataset, overall class-wise 20% data is randomly picked from the original HSI dataset using suggested spatial-spectral clustering. From the reduced HSI dataset, 80% and 20% of the data were randomly split into training and testing groups, respectively. Tables 2, 3, and 4 exhibit the classification results for IP, PU, and SA datasets, respectively. The number of trainable parameters in the Hybrid-LN model is significantly lower than 3D-CNN model, as shown in Table 5. Tables 2 through 4 show a comparison of the classification accuracies of various techniques. Based on the findings from the IP dataset, it can be shown that the suggested model's classification accuracy is higher in terms of average accuracy (AA), overall accuracy

(OA), and kappa (K) coefficient. Based on these findings, the classification accuracy of Hybrid-LN is quite similar to that of 3D-CNN, but the number of parameters to adjust is considerably decreased, allowing the proposed approach to run with little computing resources.

No.	SVM	2D-CNN	3D-CNN	SMSB	Hybrid-LN
1	62.05	75.38	96.92	<b>100</b>	98.87
2	81.45	91.54	98.91	93.18	<b>99.4</b>
3	70.55	86.95	98.84	98.52	<b>99.52</b>
4	72.93	88.56	97.71	91.87	<b>99.03</b>
5	93.17	86.05	99.32	99.32	<b>99.68</b>
6	97.32	96.13	99.74	98.95	<b>100</b>
7	84.35	82.61	93.04	95.75	<b>100</b>
8	98.32	97.88	<b>100</b>	<b>100</b>	99.95
9	51.76	65.88	<b>100</b>	<b>100</b>	<b>100</b>
10	77.87	89.85	99.15	93.04	<b>99.39</b>
11	85.10	95.28	99.23	98.34	<b>99.78</b>
12	79.09	88.65	97.86	96.23	<b>99.82</b>
13	98.39	97.82	99.89	99.46	<b>100</b>
14	95.59	98.40	99.59	99.66	<b>99.89</b>
15	61.28	89.21	98.48	98.52	<b>99.4</b>
16	87.60	82.53	95.70	94.12	<b>98.84</b>
OA	84.48	92.69	99.08	97.21	<b>99.62</b>
AA	81.05	88.29	98.40	97.31	<b>99.6</b>
Kappa	82.26	91.65	98.95	96.81	<b>99.57</b>

Table 2. Class-wise accuracy for Indian pines data in comparison state-of-art methods.

No.	SVM	2D-CNN	3D-CNN	SMSB	Hybrid-LN
1	94.29	98.01	<b>100</b>	99.11	99.96
2	97.49	99.41	<b>100</b>	98.97	99.93
3	80.84	93.90	99.35	98.89	<b>99.77</b>
4	94.21	98.14	99.74	98.74	<b>99.73</b>
5	99.22	99.57	<b>100</b>	100	<b>100</b>
6	90.91	98.08	<b>100</b>	99.87	<b>100</b>
7	87.35	89.72	99.98	99.97	<b>100</b>
8	87.47	98.28	99.74	98.99	<b>100</b>
9	99.86	98.87	99.60	98.04	<b>99.78</b>
OA	94.10	98.27	99.92	99.11	<b>100</b>
AA	92.40	97.11	99.82	99.16	<b>99.95</b>
Kappa	92.17	97.71	<b>99.89</b>	98.79	<b>99.86</b>

Table 3. Class-wise accuracy for Pavia university data in comparison state-of-art methods.

No.	SVM	2D-CNN	3D-CNN	SMSB	Hybrid-LN
1	99.63	99.45	<b>100</b>	99.78	99.2
2	99.91	99.51	<b>100</b>	99.97	<b>100</b>
3	99.68	99.62	<b>100</b>	99.94	99.8
4	99.31	99.89	99.86	99.28	<b>100</b>
5	99.35	99.88	99.95	99.54	<b>100</b>
6	99.80	99.78	<b>100</b>	99.97	<b>100</b>
7	99.54	99.64	<b>100</b>	98.88	<b>100</b>
8	90.51	95.60	<b>99.97</b>	98.87	99.75
9	99.92	99.54	<b>100</b>	99.91	<b>100</b>
10	97.71	98.45	<b>99.99</b>	98.85	99.4
11	98.88	98.73	<b>100</b>	99.79	<b>100</b>
12	99.79	99.58	99.99	99.94	<b>100</b>
13	98.88	99.13	99.98	99.03	<b>100</b>
14	97.65	97.53	99.98	98.86	<b>100</b>
15	70.54	95.01	99.95	97.63	99.96
16	99.18	97.00	<b>99.94</b>	99.92	99.28
OA	93.67	97.94	99.98	99.26	<b>99.99</b>
AA	96.89	98.65	99.98	99.45	<b>99.98</b>
Kappa	92.94	97.71	<b>99.98</b>	99.17	99.72

Table 4. Class-wise accuracy for Salinas data in comparison state-of-art methods.

Dataset	2D-CNN	3D-CNN	Hybrid-LN
IP	378116	1805196	<b>688240</b>
PU	377409	1803089	<b>688009</b>
SA	378116	1805196	<b>688240</b>

Table 5. Comparisons with respect to the number of trainable parameters on the three HSI datasets.

## 5. Conclusion

For HSI classification, this article proposes a hybrid learning technique for feature extraction and classification (Hybrid-LN) framework. By decreasing the size of the original HIS dataset, it is a straightforward two-step approach that extracts both spatial and spectral information from the HSI dataset. The first stage reduces the spatial-spectral information by clustering the HSI pixels and spectral bands, resulting in spatial-spectral reduced HSI data. The HSI classification is performed in the second phase, which involves training a CNN to extract spatial-spectral features. To decrease computational complexity, this framework can handle large-scale datasets. The proposed Hybrid-LN technique is tested against four state-of-the-art deep learning-based HSI classification techniques on three publicly accessible benchmark datasets. The suggested Hybrid-LN framework produced reasonably excellent performance with fewer parameters, as demonstrated in experiments.

## References

- [1] Bioucas-Dias, J. M; Plaza, A; Camps-Valls, G; Scheunders, P; Nasrabadi, N; Chanussot, J, (2013): Hyperspectral remote sensing data analysis and future challenges, *IEEE Geoscience and remote sensing magazine*, vol. 1, no. 2, pp. 6–36.
- [2] Cariou, C; Chehdi, K; Moan, S. L, (2020): Improved nearest neighbor density-based clustering techniques with application to hyperspectral images, in *ICASSP 2020 - 2020 IEEE International Conference on Acoustics, Speech and Signal Processing (ICASSP)*, pp. 4127–4131.
- [3] Okwuashi, o; Ndehedehe, C. E, (2020): Deep support vector machine for hyperspectral image classification, *Pattern Recognition*, p. 107298.
- [4] Xu, H; Zhang, H; He, W; Zhang, L, (2019): Supapixel-based spatialspectral dimension reduction for hyperspectral imagery classification, *Neurocomputing*, vol. 360, pp. 138–150.
- [5] Cao, X; Wei, C; Ge, Y; Feng, J; Zhao, J; Jiao, L, (2019): Semi-supervised hyperspectral band selection based on dynamic classifier selection, *IEEE Journal of Selected Topics in Applied Earth Observations and Remote Sensing*, vol. 12, no. 4, pp. 1289–1298.
- [6] Aria, S. E. H; Menenti, M; Gorte, B. G; Homayouni, S, (2020): Unsupervised dimensionality reduction of hyperspectral images using representations of reflectance spectra, *International Journal of Remote Sensing*, vol. 41, no. 20, pp. 7820–7845.
- [7] Paoletti, M; Haut, J; Plaza, J; Plaza, A, (2019): Deep learning classifiers for hyperspectral imaging: A review,” *ISPRS Journal of Photogrammetry and Remote Sensing*, vol. 158, pp. 279–317.
- [8] Hamouda, M; Ettabaa, K. S; Bouhlef, M. S, (2020): Smart feature extraction and classification of hyperspectral images based on convolutional neural networks, *IET Image Processing*, vol. 14, no. 10, pp. 1999–2005.
- [9] Wei, Y; Niu, C; Wang, Y; Wang, H; Liu, D, (2019): The fast spectral clustering based on spatial information for large scale hyperspectral image, *IEEE Access*, vol. 7, pp. 141045–141054.
- [10] Datta, A; Ghosh, S; Ghosh, A, (2012): Clustering based band selection for hyperspectral images, in *2012 international conference on communications, devices and intelligent systems (CODIS)*, pp. 101–104, IEEE.
- [11] Yao, W; Lian, C; Bruzzone, L, (2020): Clustercnn: Clustering-based feature learning for hyperspectral image classification, *IEEE Geoscience and Remote Sensing Letters*.
- [12] Bianca B. L; Gheorghe, P. S, (2014): Unsupervised clustering for hyperspectral images, *Symmetry*, vol. 12, no. 2, p. 277, 2020.
- [13] Xu, L; Li, J; Wong, A; Peng, J, (2014): Kp-means: A clustering algorithm of k “purified” means for hyperspectral endmember estimation. *IEEE Geoscience and Remote Sensing Letters* 11.10 1787–1791.
- [14] Kumar, V. S; Naganathan, E; Sivaprakasam, S. A; Kavitha, M, (2020): Robust k-means technique for band reduction of hyperspectral image segmentation, in *Applications of Hybrid Metaheuristic Algorithms for Image Processing*, pp. 81–103, Springer.
- [15] Kennedy, S. M; Williamson, W; Roth, J. D; Scrofani, J. W, (2020): Cluster-based spectral-spatial segmentation of hyperspectral imagery, *IEEE Access*, vol. 8, pp. 140361–140391.
- [16] Tremblay, N and Loukas, A, (2020): Approximating spectral clustering via sampling: a review, in *Sampling Techniques for Supervised or Un-supervised Tasks*, pp. 129–183, Springer.
- [17] Challa, A; Danda, S; Sagar, B. D; Najman, L, (2020): Power spectral clustering, *Journal of Mathematical Imaging and Vision*, pp. 1–19.
- [18] Liu, Y; Cai, Y; Yang, X; Nie, F; Ye, W, (2020): Fast adaptive neighbors clustering via embedded clustering, *Neurocomputing*.
- [19] Yuan, M. and Zhu, Q. (2020): Spectral clustering algorithm based on fast search of natural neighbors, *IEEE Access*, vol. 8, pp. 67277–67288.
- [20] Li, Y; Zhang, H; Shen, Q, (2017): Spectral–spatial classification of hyperspectral imagery with 3d convolutional neural network, *Remote Sensing*, vol. 9, no. 1, p. 67.
- [21] Hao, S; Wang, W; Yan, Y; Bruzzone, L, (2017): Class-wise dictionary learning for hyperspectral image classification, *Neurocomputing*, vol. 220, pp. 121–129.
- [22] Yu, S; Jia, S; Xu, C, (2017): Convolutional neural networks for hyperspectral image classification, *Neurocomputing*, vol. 219, pp. 88–98.
- [23] Liu, B; Yu, X; Zhang, P; Yu, A; Fu, Q; Wei, X, (2017): Supervised deep feature extraction for hyperspectral image classification, *IEEE Transactions on Geoscience and Remote Sensing*, vol. 56, no. 4, pp. 1909–1921.
- [24] Paoletti, M; Haut, J; Plaza, J; Plaza, A, (2018): A new deep convolutional neural network for fast hyperspectral image classification, *ISPRS journal of photogrammetry and remote sensing*, vol. 145, pp. 120–147.
- [25] Chen, C; Jiang, F; Yang, C; Rho, S; Shen, W; Liu, S; Liu, Z, (2018): Hyperspectral classification based on spectral–spatial convolutional neural networks, *Engineering Applications of Artificial Intelligence*, vol. 68, pp. 165–171.
- [26] Zhang, P; He, H; Gao, L, (2019): A nonlinear and explicit framework of supervised manifold-feature extraction for hyperspectral image classification, *Neurocomputing*, vol. 337, pp. 315–324.
- [27] Yu, C; Han, R; Song, M; Liu, C; Chang, C.-I, (2020): A simplified 2d-3d cnn architecture for hyperspectral image classification based on spatial-spectral fusion, *IEEE Journal of Selected Topics in Applied Earth Observations and Remote Sensing*.
- [28] Azar, S. G; Meshgini, S; Rezaei, T. Y, Beheshti, S, (2020): Hyperspectral image classification based on sparse modeling of spectral blocks, *arXiv*, pp. arXiv–2005.
- [29] Fang, J. and Cao, X, (2020): Multidimensional relation learning for hyperspectral image classification, *Neurocomputing*, vol. 410, pp. 211–219.



- [30] Yuan, Y; Zheng, X; Lu, X; (2016): Discovering diverse subset for unsupervised hyperspectral band selection, IEEE Transactions on Image Processing, vol. 26, no. 1, pp. 51–64.
- [31] Wu, M; Zhao, Y; Zhang, L; Wang, J; Xu, H; Wei, D; (2017): Ensemble clustering model of hyperspectral image segmentation, in 2017 9th International Conference on Advanced Infocomm Technology (ICAIT), pp. 356–360, IEEE.
- [32] Wang, Q; Zhang, F; Li, X, (2018): Optimal clustering framework for hyperspectral band selection, IEEE Transactions on Geoscience and Remote Sensing, vol. 56, no. 10, pp. 5910–5922.
- [33] Xie, H, Zhao, A, Huang, S, Han, J, Liu, S, Xu, X; Luo, X; Pan, H; Du, Q, Tong, X, (2018): Unsupervised hyperspectral remote sensing image clustering based on adaptive density, IEEE Geoscience and Remote Sensing Letters, vol. 15, no. 4, pp. 632–636.
- [34] Zhao, Y; Yuan, Y; Wang, Q. (2019): Fast spectral clustering for unsupervised hyperspectral image classification, Remote Sensing, vol. 11, no. 4, p. 399.

## Authors Profile



Murali Kanthi received the B.Tech. degree from JNTUA College of Engineering, Anantapur, Andhra Pradesh in 2007 and the M.Tech degree from JNTUA College of Engineering, Anantapur, Andhra Pradesh in 2009, where he is currently pursuing the Ph.D. degree in computer science and engineering. His research areas include Machine Learning, Hyperspectral Image Processing, Data Mining, and Deep Learning.



Dr. T. Hitendra Sarma obtained Ph.D. in Machine Learning from JNT University, Anantapur, Andhra Pradesh, India in the year 2013. He is a recipient of the Teachers Associateship for Research Excellence (TARE) grant by SERB-DST Govt. of India. He has published more than 25 articles in peer-reviewed Journals and reputed international conferences like IJCNN, CEC, PReMI and others. He delivered an invited at FSDM -2017 in Taiwan. He is a senior member of IEEE. His research areas include Machine Learning, Hyperspectral Image Processing and Data Mining.



Dr. C. Shoba Bindu, Ph.D. in CSE from JNTUA, Anantapuramu, Andhra Pradesh. She is currently working as a Professor in the Department of CSE, JNTUA College of Engineering, Ananthapuramu. Her research areas include Computer Networks, Network Security, Machine Learning, and Cloud Computing.